Auto-adjoint time domain elastic full waveform inversion

Tianze Zhang*, Kris Innanen, Daniel Trad, Jian Sun
zhang.tianze@ucalgary.ca

Abstract

We propose the Auto-adjoint time domain elastic full waveform inversion in this report, which is a FWI framework accelerated with CUDA using adjoint sources calculated with automatic differential method. In this FWI framework, the forward modeling and the adjoint modeling are accelerated by CUDA, and the adjoint sources are calculated by the automatic differential method. These two features allows us to perform time domain FWI with GPU acceleration and explore how different kinds of objective functions can influence the inversion results effectively. We study the objective function behavior for the $\ell 2$ norm, $\ell 1$ norm, Global-correlation based, Envelope based, objective function, and $\ell 1$ norm between the real and imaginary part of the synthetic data and the observed data ($\ell 1$ RI objective function). According to the numerical test we did in this paper, the $\ell 1$ RI objective function has better ability to tolerate the noise when poor initial model is used for inversion, compared with all the other objective functions we considered.

Introduction

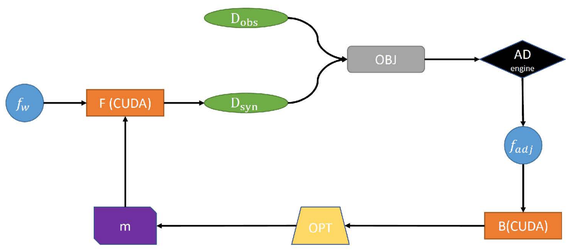

FIG. 1. The inversion framework of Auto-adjoint EFWI. D_{syn} and D_{obs} are the synthetic data and observed data respectively. OBJ is the objective function value calculated according to the objective function we choose. AD engine is the automatic differential engine which is used to calculate the adjoint sources for backpropagation. B stands for the backpropagation operator. which is accelerated by CUDA, which is also programmed in the form of the RNN. OPT is the optimization method which gives the direction for the elastic models for model updating

Table 1. Objective functions provided

Name	Acronym	Expression $\mathcal{X}$
$\ell 2$ norm	WD	$\frac{1}{2}\sum_{\mathbf{x}_r}\int_0^T \|\|\mathbf{d}_{\text{syn}}(\mathbf{x}_r,t,\mathbf{m})-\mathbf{d}_{\text{obs}}(t)\|\|^2 \text{dt}$
$\ell 1$ norm	ABSWD	$\sum_{\mathbf{x}_r}\int_0^T \|\|\mathbf{d}_{\text{syn}}(\mathbf{x}_r,t,\mathbf{m})-\mathbf{d}_{\text{obs}}(\mathbf{x}_r,t,\mathbf{m})\|\| \text{dt}$
Huber norm	HWD	$\begin{cases}\frac{1}{2}\sum_{\mathbf{x}_r}\int_0^T \|\|\mathbf{d}_{\text{syn}}(\mathbf{x}_r,t,\mathbf{m})-\mathbf{d}_{\text{obs}}(t)\|\|^2 \text{dt}, & \text{if } \|\alpha\|\le\epsilon \\ \sum_{\mathbf{x}_r}\int_0^T \|\|\mathbf{d}_{\text{syn}}(\mathbf{x}_r,t,\mathbf{m})-\mathbf{d}_{\text{obs}}(\mathbf{x}_r,t,\mathbf{m})\|\| \text{dt}, & \text{if } \|\alpha\|>\epsilon\end{cases}$ α is the absolute difference between observed data and synthetic data. ϵ is a hyper-parameter threshold.
Global Correlation	GC	$-\sum_{\mathbf{x}_r}\int_0^T \frac{\mathbf{d}_{\text{syn}}(\mathbf{x}_r,t,\mathbf{m})*\mathbf{d}_{\text{obs}}(t)}{\sqrt{E_{\text{obs}}E_{\text{syn}}}}\text{dt}$,where the E_{obs} and E_{syn} are the energy of the trace. $E_{\text{obs}}=\int_0^T \mathbf{d}_{\text{obs}}^2(t)\text{dt}$. $E_{\text{syn}}=\int_0^T \mathbf{d}_{\text{syn}}^2(\mathbf{x}_r,t,\mathbf{m})\text{dt}$.
Zero mean Global Correlation	ZMGC	$-\sum_{\mathbf{x}_r}\int_0^T \frac{(\mathbf{d}_{\text{syn}}(\mathbf{x}_r,t,\mathbf{m})-\bar{d}_{obs})*(\mathbf{d}_{\text{obs}}(t)-\bar{d}_{syn})}{\sqrt{E_{\text{robs}}E_{\text{rsyn}}}}\text{dt}$. $E_{\text{robs}}=\int_0^T(\mathbf{d}_{\text{obs}}(t)-\bar{d_{\text{obs}}})^2\text{dt}$. $E_{\text{rsyn}}=\int_0^T(\mathbf{d}_{\text{syn}}(\mathbf{x}_r,t,\mathbf{m})-\bar{d_{\text{syn}}})^2\text{dt}$. $\bar{d_{syn}}$ and $\bar{d_{obs}}$ are the mean value of the traces.
$\ell 1$ real and imaginary	$\ell 1$ RI	$\sum_{\mathbf{x}_r}\int_0^{\omega_{max}} \|\|\Re(\mathcal{F}_{\text{syn}})-\Re(\mathcal{F}_{\text{obs}})\|\|+\|\|\Im(\mathcal{F}_{\text{syn}})-\Im(\mathcal{F}_{\text{obs}})\|\|\text{d}\omega$, where $\mathcal{F}_{\text{syn}}$ and $\mathcal{F}_{\text{obs}}$ are the FFT of $\mathbf{d}_{\text{syn}}$ and $\mathbf{d}_{\text{obs}}$. $\Re$ stands for real part. $\Im$ stands for imaginary part.
Envelope	EN	$\frac{1}{2}\sum_{\mathbf{x}_r}\int_0^T \|\|\mathcal{A}_{\text{syn}}(\mathbf{x}_r,t,\mathbf{m})-\mathcal{A}_{\text{obs}}(t)\|\|^2\text{dt}$, where $\mathcal{A}_{\text{syn}}$ and $\mathcal{A}_{\text{obs}}$ are the envelope of $\mathbf{d}_{\text{syn}}$ and $\mathbf{d}_{\text{obs}}$.
Multi-scale Z transform	MZ	$\frac{1}{2}\sum_{\mathbf{x}_r}\int_0^{\omega_{max}} \|\|\Re(\mathcal{Z}_{\text{syn}})-\Re(\mathcal{Z}_{\text{obs}})\|\|^2\text{d}\omega$, where $\mathcal{Z}_{\text{syn}}$ and $\mathcal{Z}_{\text{obs}}$ are the discrete Z transform of $\mathbf{d}_{\text{syn}}$ and $\mathbf{d}_{\text{obs}}$ with damping coefficient $z_d>1$.

Numerical tests

Marimousi model inversion test

- The grid length of the model is 30 × 30.
- The grid size of the model is 130 × 225.
- Time interval dt = 0.002s.
- Maximum receiving time 2.6s.
- Ricker's wavelet 10 Hz main frequency.
- Ocean Bottom Cable (OBC) acquisition system.
- Maximum iteration time 500.
- Adam's algorithm.

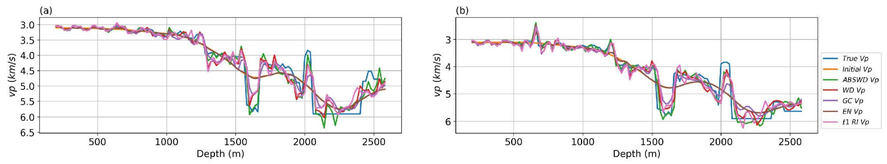

FIG. 2. V_p vertical profiles

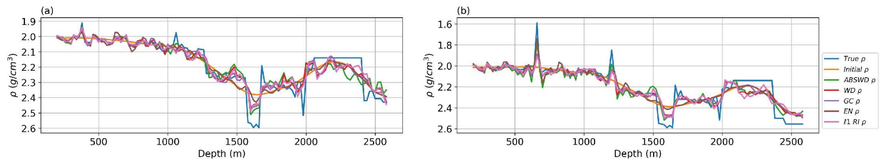

FIG. 3. V_s vertical profiles

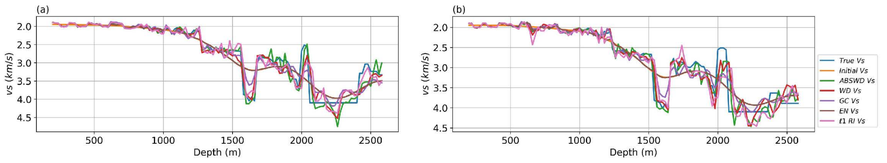

FIG. 4. ρ vertical profiles

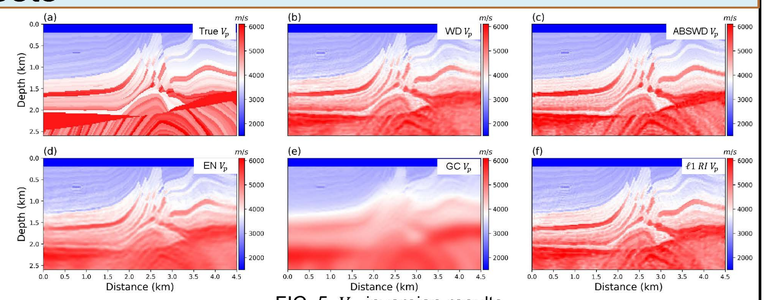

FIG. 5. V_p inversion results

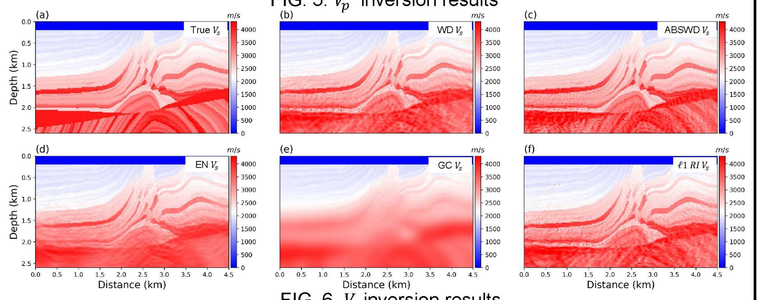

FIG. 6. V_s inversion results

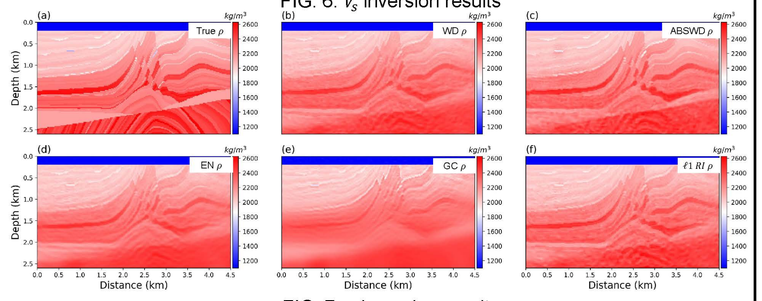

FIG. 7. ρ inversion results

Stress noise inversion test (SNR=10dB)

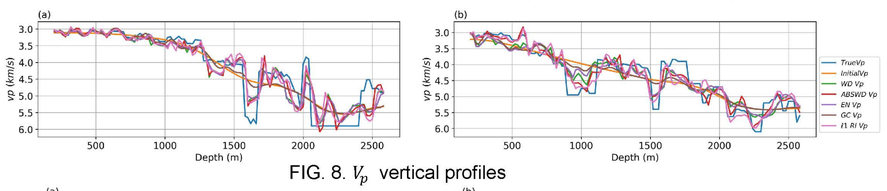

FIG. 8. V_p vertical profiles

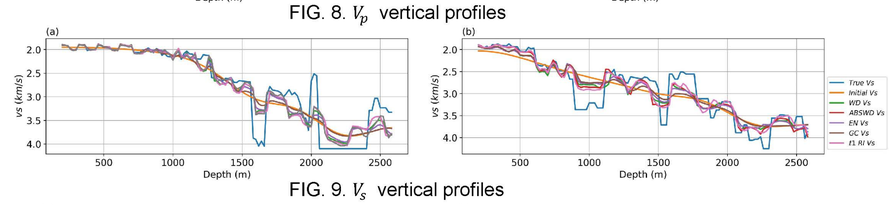

FIG. 9. V_s vertical profiles

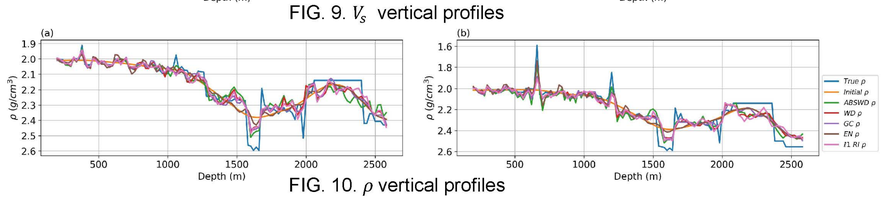

FIG. 10. ρ vertical profiles

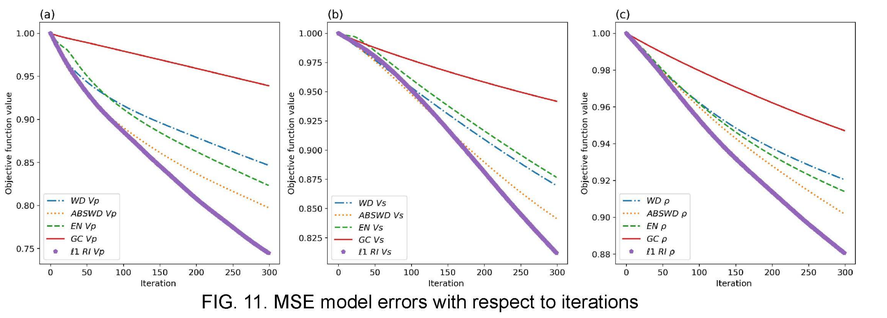

FIG. 11. MSE model errors with respect to iterations

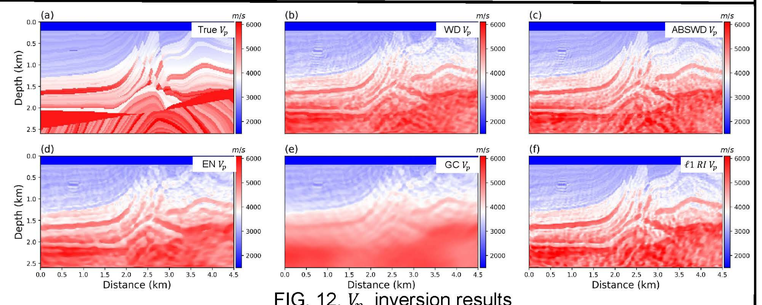

FIG. 12. V_p inversion results

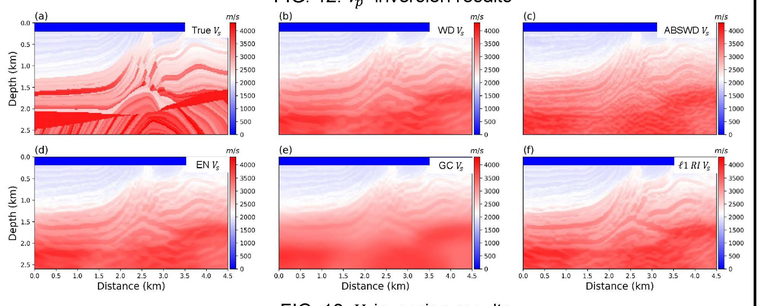

FIG. 13. V_s inversion results

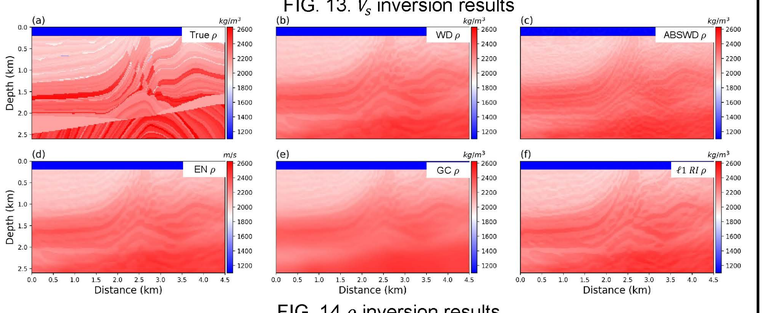

FIG. 14. ρ inversion results

NSERC CRSNG
UNIVERSITY OF CALGARY
FACULTY OF SCIENCE
Department of Geoscience